In-situ quality control of structural strengthening by epoxy-bonded CFRP strips

Claus Germann Petersen
President, Germann Instruments, Inc., 8845 Forest View Road, Evanston. Illinois 60203, USA.
E-mails: germann@post6.tele.dk and germann@interaccess.com

Ervin Poulsen
Professor Emeritus of C.Eng., 8 Skovbrynet, Nodebo. DK-3480 Fredensborg, Denmark.
E-mail: ervin-poulsen@get2net.dk

ABSTRACT: According to CEN ENV 1504 on 'Products and systems for the protection and repair of concrete structures' – Part 9: 'General principles for the use of products and systems' and Part 10: 'Site application of products and systems and quality control of the works' there is a minimum of requirements before the strengthening of a structural component can take place and of the quality control of the strengthening. The purpose is to control the work before, during and after the strengthening of a RC concrete structural component by structural bonding by CFRP strips.

The paper describes several test methods which can be applied in connection with in-situ quality control of the strengthening of RC structures by epoxy bonded CFRP strips.

1 INTRODUCTION

In details the in-situ control testing of RC structures, strengthened by epoxy bonded CFRP strips includes:

- Inspection and control testing of the near-to-surface layer of concrete to which the CFRP strips have to be glued by adhesive, e.g.:
  - Delamination and similar defects
  - Cracks and texture of the concrete surface (substrate)
  - Carbonation depth of substrate
  - Chloride ingress into substrate
  - Corrosion rate of the existing reinforcement by the GalvaPulse test method.
- Strength of the near-to-surface layer of the substrate concrete, e.g.:
  - Pull-off strength of the substrate
  - Pure shear strength of the substrate
  - Ultimate anchorage force of a CFRP strip bonded to the substrate.
- Defects and slip of bonded CFRP strips, e.g.:
  - Impact-echo inspection to detect defects and cavities encapsulated by the adhesive.

The paper describes how well-known in-situ test methods have been modified in order to serve as in-situ test methods of inspection of the quality of epoxy-bonded CFRP strips as a strengthening system for the upgrading of RC structures. The in-situ methods of impulse-response, impact echo, carbonation, chloride, corrosion rate, pull-off test, DSS-test, in-situ. are described, and it is demonstrated how the methods are applied in practice for the control testing of strengthening of RC structures by CFRP strips.

2 IN-SITU TEST METHODS

2.1 *Flaw screening by s'MASH Impulse-Response*

With the s'MASH testing method slabs, columns and walls are screened non-destructively for dynamic mobility, foolproof and very quickly, cf. Figure 1.

Figure 1. The s'MASH used for detection of the dynamic stiffness of a structural RC member.

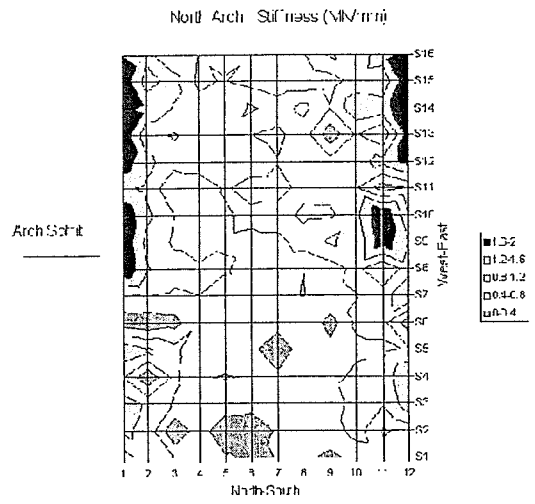

Figure 2. The dynamic stiffness measured with the s'MASH Impulse Response System of an arc bridge.

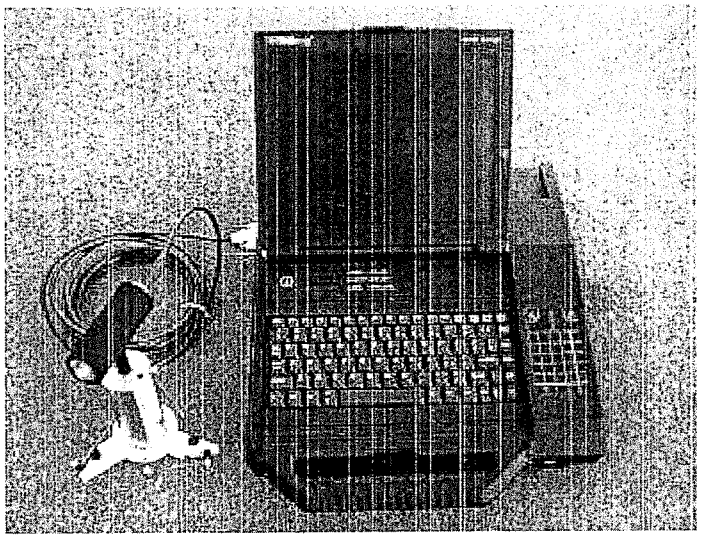

Figure 3. The DOCter Mark IV transducer unit with the field computer for thickness measurement and flaw detection.

One of the parameter in a mobility plot, cf. *Davis et al* (1959), is the dynamic stiffness, which in turn indicate the presence of voids, cracking, honeycombs, ASR and delaminating concrete around steel reinforcement. The system is also powerful for detecting the degree of stress transfer through load transfer systems, e.g. across joints in concrete structural members.

An impulse is used to send a stress wave through the tested element by means of a 1-kg sledgehammer with a built-in load cell in the hammerhead. The member tested will respond in a bending mode over a low frequency range (0-1 kHz for plates). The response is picked up by a velocity transducer (geophone) positioned on the surface adjacent to the hammer impulse location. Both the hammer and the geophone are connected to a portable field computer with data acquisition card and impulse-response software.

The time records for the hammer force and the geophone velocity are processed in the computer using the Fast Fourier Transform (FFT) algorithm. The resulting velocity spectrum is divided by the force spectrum to obtain a transfer spectrum - the Mobility Graph - of the element. The graph plotted against frequency contains information of the condition and the integrity of the member, such as the dynamic stiffness.

Test data is processed immediately on-site and presented as contour charts for easy and quick comparative identification of areas requiring further detailed investigation. An example of such a chart from an arch bridge is shown in Figure 2.

2.2 *Position of flaws with DOCter Impact-Echo*

The s'MASH impulse-response system will allow large areas to be screened quickly followed up by detailed analysis in critical areas by the DOCter impact-echo system, cf. Figure 3.

The impact-echo, cf. *Sansalone et al* (1998), uses reflection of the stress wave submitted by impact to detect the depth of anomalies in the concrete member, such as delaminations, honeycombing, debonding, cracking and voids, ASR and air in cable ducts. In addition, the system measures non-destructively the thickness of concrete members within ± 1.5 %, cf. *Sansalone et al* (1998).

An impact is given to the surface with a spherical steel impactor. The impactor is selected from a variety of impactors with diameters of 3 mm, 5 mm, 6.5 mm, 8 mm, 9.5 mm, 12 mm and 15 mm. The stress wave traveling into the member will be reflected from a material inside the member with a different acoustic impedance, e.g. air, return to the surface, be reflected again, etc. The arrival of the stress wave (the P-wave) to the surface is picked up by a sensitive displacement transducer placed close to the impactor and analyzed into frequency by means of the Fast Fourier Transform (FFT) algorithm.

For reflection from a material with less acoustic impedance the depth D is determined by:

$$D = \frac{C_p}{2f} \tag{1}$$

C_p is the wave speed and f the frequency due to reflection of the P-wave from the interface.

If the reflection is occurring from an interface with higher acoustic impedance such as steel, the following equation applies:

$$D = \frac{C_p}{4f} \tag{2}$$

For a 3 mm impactor the frequency range detected is approximately 1.2 kHz to 80 kHz and for a 15 mm impactor 1.2 kHz to 15 kHz. The 3 mm impactor will be able to detect defects with a minimum lateral

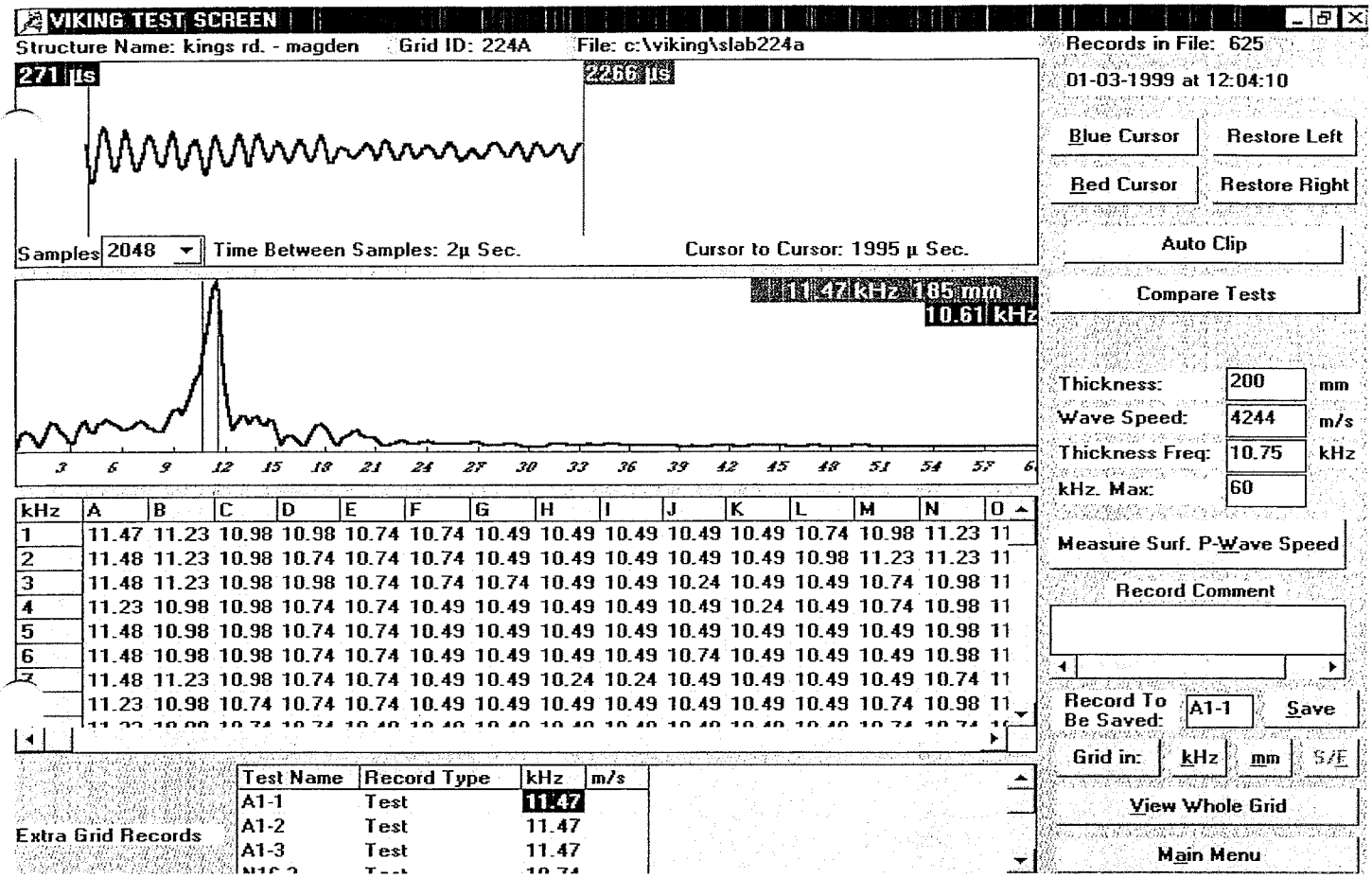

Figue 4. Impact-echo record indicating the depth of 185 mm to an air refection interface.

size of 40 mm, positioned minimum 20 mm deep and maximum 80 mm deep. Similarly, at the other end of the impactor range, the 15 mm impactor will detect defects with a minimum lateral size of approx. 250 mm positioned minimum 125 mm and maximum 1000 mm deep.

An example of a test record indicating the depth to an air reflection interface at 185 mm of a 200 mm plate is shown in Figure 4. The P-wave speed was, prior to the measurement, measured by two Mark IV transducers placed on the surface. The P-wave speed measured was 4244 m/s.

2.3 *Carbonation testing with Rainbow Indicator*

A core, 13 mm in diameter and appx. 60 mm deep, is drilled out using a handheld water cooled coring device. The core is sprayed with the Rainbow Indicator and allowed to dry. The emerging colors will give the pH-values of the concrete from the surface towards the reinforcement according the following scale:

Table 2. Color of concrete vs. pH-value

Color	pH-value
Orange	5
Yellow	7
Green	9
Purple	11
Dark blue	13

The Rainbow Indicator has been shown to be as accurate for detection of the depth of carbonation (starting point of the green color) as thin-section analysis, cf. *Cambell et al* (1991).

2.4 *Chloride testing with RCT*

With the RCT the acid soluble amount of chlorides is measured in percentage of concrete mass, on-site. The equipment comes in a portable attaché case.

Concrete powder is drilled out using an 18 mm drill bit and a collecting pan. For maximum aggregate size of up to 32 mm approximately twenty grams of dust have to be obtained for eliminating the influence of the aggregates on the testing for chlorides. This is for depth increments of 5 mm towards the reinforcement achieved by drilling at three locations adjacent to each other.

For evaluation of the chloride profile towards the reinforcement practice has been, cf. Henriksen et al (1993), to collect the first powder sample in the outer non-carbonated concrete layer, the second in the middle and a third at the depth of the reinforcement.

Alternatively, the powder sampling may be done at exact depth increments (between 1 and 2 mm) using the Profile Grinder, on-site, cf. *Petersen et al* (1995).

From the powder samples 1.5 gram of powder is weighed using a simple volumetric method. The weighed powder is poured into a vial with 10 ml of extraction liquid. After five minutes of shaking of the vial a calibrated chloride sensitive is submerged into the solution and the reading in mV taken on a connected mV-meter. The measurements in mV are

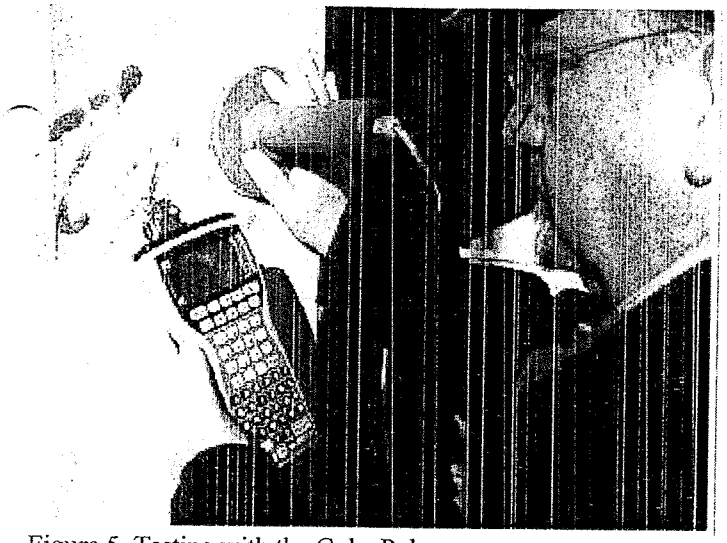

Figure 5. Testing with the GalvaPulse.

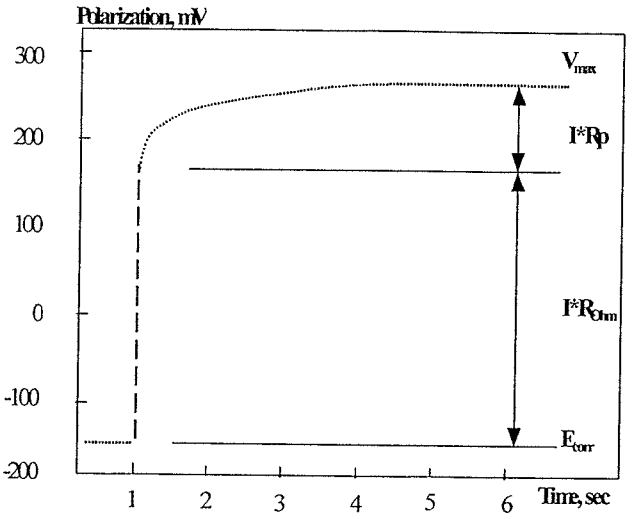

Figure 6. Typical polarization pattern for a corroding bar.

plotted on a calibration sheet giving the acid soluble amount of chlorides.

The five minutes of shaking of the vial will not extract all the acid soluble chlorides. For accurate measurements a correction factor is applied (1.05 to 1.10) depending on the chloride level, cf. *Henriksen et al* (1993). Alternatively, leaving the vial standing over night will extract all the acid soluble chlorides in the solution.

In comparison to reference concrete powders with known amounts of chlorides the RCT has been shown to be as accurate as AASHTO T 260 standard potentiometric titration, cf. *Petersen* (1999).

The concrete powders produced by The Swedish National Testing Institute (SP) have different types of cements (Portland, Flyash and Slag Cement) and have chloride contents from 0.020% to 0.328% by mass concrete.

In comparison to the known amount of the chlorides in these concrete powders the total variation of the RCT was found to be ± 4 %, cf. *Petersen* (1999).

2.5 *Corrosion activity with GalvaPulse*

The GalvaPulse measures the corrosion rate of the reinforcement as well as the half-cell potentials and the electrical resistance of the cover layer.

For on-site measurement two modes are available, either for half-cell & electrical resistance or half-cell & corrosion rate & electrical resistance. One set of measurements in the first mode last half a second and in the second mode 5-10 seconds, normally.

Before measurement starts out the reinforcement in the measuring area is checked for electrical continuity. The testing is illustrated in Figure 5 and a typical polarization pattern in Figure 6.

The electrode contains a guard ring, a counter electrode and a reference electrode.

At first, the free half-cell potential and the electrical resistance are measured between the electrode and the reinforcement.

Subsequently, for the corrosion rate a pre-set current pulse is applied over time to the reinforcement, the potential-time curve recorded as illustrated in Figure 6, and the polarization resistance R_p calculated. By means of the Stern Geary equation:

$$I_{corr} = \frac{25}{R_p} \tag{3}$$

the corrosion current I_{corr} is estimated. For a known confined area A of the reinforcement the corrosion rate CR can be evaluated according to Faraday's Law of electrical equivalence as:

$$CR = 11.6 \times \frac{I_{corr}}{A} \tag{4}$$

where

- CR is the corrosion rate in µm/year (i.e. 0.001 mm/year)
- 11.6 is a Factor relating the corrosion current to loss of cross section for black steel
- I_{corr} Corrosion current in µA
- A is the confined reinforcement area in cm^2

Measurements are stored in a predetermined grid (max. 99 × 99 points per file) in the handheld mini computer and transferred to a home office computer for printout of the half-cell potentials, corrosion rate and electrical resistance in 2- or 3-dimensions color plots.

The GalvaPulse and on-site measurements are described in detail by *Klinghoffer et al* (1999). The GalvaPulse measurements were found to correlate faveroubly to corrosion current measured by post mounted sensors. In addition, initiation of high corrosion rates was clearly demonstrated over a six year period of 30 years old bridge pillars subjected to deicing salts.

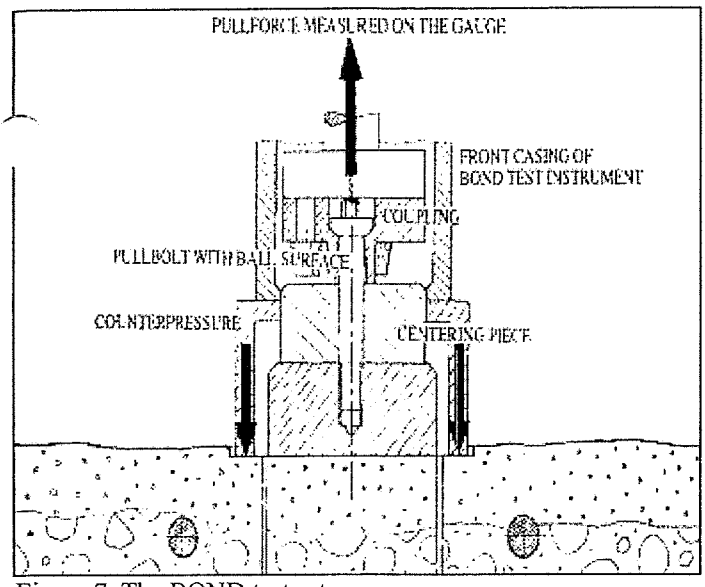

Figure 7. The BOND test set up.

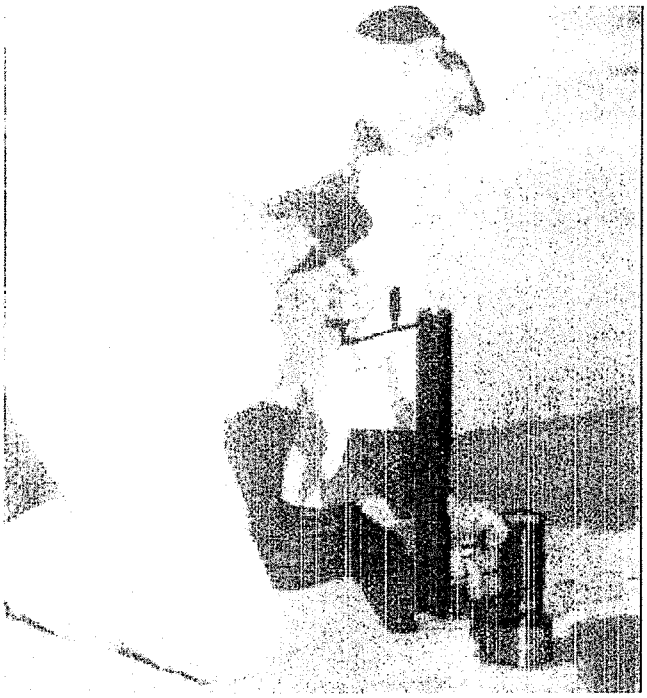
Figure 8. The BOND-test in progress.

2.6 *Tensile strength with BOND-test*

75 mm in diameter or a 50 mm steel disc is glued on to the prepared, planed surface with a quick setting two-component glue. A slot is drilled into the substrate with water-cooled coring equipment containing a diamond drill bit that fits the steel disc. The coring equipment ensures a straight drilled partial core perpendicular to the planed surface.

The disc is connected to a high tensile pull bolt with a centering plate and a coupling. The coupling is connected to a precision hydraulic pull machine resting against a circular counter pressure on the planed surface, cf. Figure 7.

Loading takes place with a constant loading rate until rupture of the concrete, cf. Figure 8.

2.7 *Shear strength with TORQ-test*

disc with an inner diameter of 55 mm and an outer diameter of 70 mm is glued to the surface with quick setting 2-component glue. Alternatively, prior to gluing on of the disc, two circular slots can be drilled in the surface matching the inner and outer diameters of the disc.

The disc is twisted off by means of an attached housing with eccentric loading rod connected to a hydraulic pull machine, cf. *Petersen et al* (1997).

2.8 *Shear strength of CFRP strips with DSS-test*

A CFRP strip is glued to the surface of the concrete member in question. The strip has to be glued on perpendicular to and edge and extending 200 mm from the edge.

A pedestal is fitted to the strip and anchored to the concrete member. Two jaws are afterwards glued to the extending CFRP strip and kept in position by four transverse fasteners.

A counter pressure is inserted over the jaws and transverse fasteners, resting against the pedestal. A coupling is attached to the jaws, cf. Figure 10.

The hydraulic pull machine is attached to the coupling and pulling of the strip, takes place until rupture of the strip or the concrete, cf. *Petersen et al* (1997). Test results using the DSS-test method is given by *Jensen et al* (1999).

3 CHARACTERISTICS OF OBSERVATIONS

According to the EN 1504-standards, the EN 206 and the Euronorm ENV 1992-1-1 the lower characteristic value shall be the 5 % fractile and the upper characteristic value shall be the 95 % fractile.

In order to determine the characteristic value of

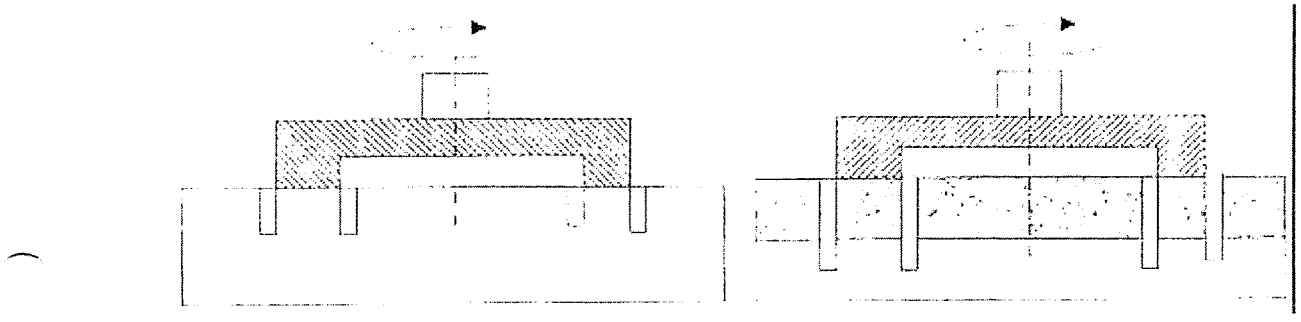
Figure 9. The TORQ-test for shear strength, left figure of the surface concrete, right figure of a CFRP strip glued to the surface. In the testing conducted it was shown that proper anchoring of the CFRP strips is essential for utilizing the full capacity of the strips.

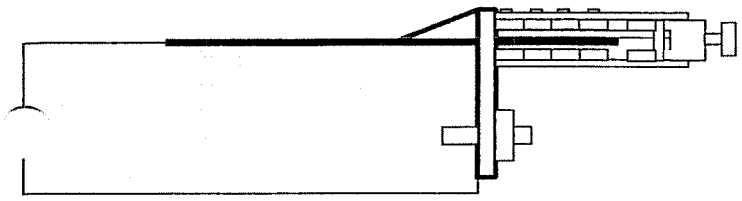

Figure 10. The DSS-test set up ready for attachment to the pull machine and shearing off of the CFRP strip.

observations it is convenient to make the following assumptions:

- Lower characteristic value is defined as the 5 % fractile.
- Upper characteristic value is defined as the 95 % fractile.
- Characteristic values shall be determined from observations at a level of confidence: $\alpha = 84.1$ %.
- Observations from testing are assumed statistically to be logarithmic normally distributed.
- The coefficient of variation is unknown.

In the case of $n \geq 3$ observations (e.g. strengths) from one single section of inspection, calculation of the characteristic value of the following observations:

$$f_1,\ f_2,\ f_3, \ldots, f_n \tag{5}$$

are carried out as follows: first the mean value $M_{\ln f}$ and the standard deviation $S_{\ln f}$ of the Napir logarithm of the observations (1), i.e. the values:

$$\ln f_1,\ \ln f_2,\ \ln f_3, \ldots, \ln f_n \tag{6}$$

are carried out. The easiest way is to apply a spreadsheet, e.g. Excel, cf. example 1. Then the lower characteristic value (5 % fractile) is:

$$f_{kl} = \exp\left(M_{\ln f} - k_n \times S_{\ln f}\right) \tag{7}$$

and the upper characteristic value (95 % fractile) is:

$$f_{ku} = \exp\left(M_{\ln f} + k_n \times S_{\ln f}\right) \tag{8}$$

The factor k_n is based upon the non-central t-distribution and obeys the values shown in Table 1 and Figure 1.

Table 1. Values of the factor k_n in Equation (3) and (4)

n	3	4	5	6	7	8	9	10
k_n	4.11	3.28	2.91	2.70	2.57	2.47	2.40	2.34
n	10	11	12	15	20	30	50	100
k_n	2.34	2.29	2.25	2.19	2.07	1.98	1.89	1.81

EXAMPLE 2. In a 450 m^2 overlay casting the following values of pull-off strengths were determined using 75 mm diameter dollies:

1.85 1.91 1.56 1.42 1.88 1.69 MPa

Calculation of the lower characteristic value (i.e. the 5 % fractile) is carried out in the following way, applying a spreadsheet, cf. table 3:

Table 3. Calculation of the characteristic value of observed pull-off strength from 6 observations.

	Pull-off strength, f_t MPa	$\ln f_t$
f_{t1}	1.85	0.6152
f_{t2}	1.91	0.6471
f_{t3}	1.56	0.4447
f_{t4}	1.42	0.3507
f_{t5}	1.88	0.6313
f_{t6}	1.69	0.5247
Mean value	1.718	0.5356
Standard deviation	0.198	0.1187
Coefficient of variation	11.5 %	–
Lower characteristic value	1.240	–

In Table 3 the mean value and the standard deviations of the logarithms of the pull-off strengths are determined as $M_{\ln f} = 0.5356$ and $S_{\ln f} = 0.1187$ respectively. Thus, the lower characteristic value (5 % fractile) yields:

$$f_{tk} = \exp\left(M_{\ln f} - k_n \times S_{\ln f}\right) =$$
$$= \exp\left(0.5356 - 2.70 \times 0.1187\right) = 1.240 \text{ MPa}$$

4 REFERENCES

Davis, A.G. & Dunn, C.S. (1974). From theory to field experience with the nondestructive vibration testing of piles, Proc. Inst. Civ. Engrs, Part 2, 74, Dec., pp 867-875.

Campbell, D.H. & Sturm, R.D. & Kosmatka & H. (1991). Detecting Carbonation. Concrete Technology Today, Portland Cement Association, Vol.12/Number 1, March 1991.

Henriksen, C.F. & Stoltzner, E. (1993). Chloride Corrosion in Danish Road-Bridge Columns", Concrete International, August 1993.

Jensen, A.P. & Petersen, C.G. & Poulsen, E. & Ottosen, C. & Thorsen. T. (1999). On the anchorage to concrete of Sika-CarboDur CFRP strips, free anchorage, anchorage devices and test results. International congress on Creating with Concrete. Dundee, Scotland. 1999.

Klinghoffer, O. & Frolund, T. & Poulsen, E. (2000). Rebar Corrosion Rate Measurements for Service Life Estimates. Paper presented at the ACI Fall Convention to Committee 365: Practical Application of Service Life Models, 15-20th October 2000, Toronto, Canada

Petersen, C.G. & Poulsen, E. (1997). In-situ testing of near-to-surface layer of concrete and epoxy-bonded CFRP strips. US-Canada-Europe Workshop on Bridge Engineering. Dubendorf and Zurich, Switzerland, 1997.

Petersen, C.G. (1995). The Profile Grinder. Corrosion of Reinforcement, Proceedings of the Nordic Seminar in Lund. Editor: Kyosti Tuutti, Feb. 1-2, University of Lund, Sweden, Report TVBM-3064, 1995.

Petersen, C.G. (1999). RCT Reference Concrete Powders with known amount of Chlorides. Germann Instruments A/S, Emdrupvej 102, DK-2400 Copenhagen, Denmark, 1999.

Sansalone, M. & Street, W.B. (1997). Impact-Echo: Nondestructive evaluation of concrete and masonry. Bullbrier Press, Ithaca, New York, 1997.